Physicochem. Probl. Miner. Process., 60(3), 2024, 188272

http://www.journalssystem.com/ppmp

Physicochemical Problems of Mineral Processing

ISSN 1643-1049

Evaluation of a novel depressant PMAA for the separation of fluorite from calcite using NaOl as a collector

Xiaofeng Zhang [1], Qi Li [2], Wenqin Qin [1], Cheng Liu [3,4], Siyuan Yang [3,4]

[1] School of Mineral Processing and Bioengineering, Central South University, Changsha, 410083, China

[2] Department of Mining and Minerals Engineering, Virginia Polytechnic Institute and State University, Blacksburg, VA 24061, USA

[3] School of Resources and Environmental Engineering, Wuhan University of Technology, Wuhan, 430070, China

[4] Hubei Key Laboratory of Resources and Eco-Environment Geology, Hubei Geological Bureau, Wuhan, 430034, China

Corresponding authors: qinwenqing369@126.com (Wenqing Qin), liucheng309@whut.edu.cn (Cheng Liu)

Abstract: It is challenging to separate fluorite from calcite due to their same calcium activated sites on their surfaces. The copolymer of maleic and acylic acid (PMAA) was used to inhibit the calcite in the flotation of fluorite. Micro-flotation results exhibited that sodium oleate (NaOl) had a good ability to collect fluorite and calcite in the scope of pH 7-10. The PMAA treatment prior to NaOl selectively depressed the floatability of calcite while allowed the flotation of fluorite, and the artificial minerals mixture plotted that fluorite/calcite could be effectively separated in the presence of PMAA/NaOl. Zeta potential results suggested that NaOl collector was absorbed on the PMAA-conditioned calcite surface but did not adsorb on the PMAA-conditioned fluorite surface. XPS results and calculational chemistry revealed the chemical interaction occurred between calcite surface and PMAA which was attributed to the calcium ions of calcite surface interacting with -COOH group of PMAA.

***Keywords*:** fluorite, calcite, NaOl collector, PMAA depressant, flotation separation

1. Introduction

Fluorite (CaF_2) can be used as the primary source of fluorine extraction, and it is a crucial non-metallic mineral in our life (Pelham 1985; Gao et al., 2019; Liu et al., 2019a). It is widely used as an important mineral raw material in the fields of the aerospace, metallurgy, hydrogen fluoride production, ceramic, and the military due to its irreplaceable properties (Seredenko et al., 1992; Gao, et al., 2021; Wang et al., 2021a). Hence, fluorite was listed as a "strategic mineral resource" in some countries, such as China, Europe, and America (Tang, 2010). Currently, the utilization of medium and low-grade fluorite ores is becoming increasingly attractive due to the depletion of high-quality fluorite ore (Fang et al., 2014). Therefore, processing medium and low-grade fluorite is for producing a product with market value.

In nature, fluorite usually associates with sulphide minerals (Liu et al., 2019b; Ye and He, 2005), barite (Liu et al., 2019a), calcite and quartz (Ye and Lu, 2021), scheelite (Gao et al., 2015; He et al., 2022). Forth flotation is commonly used to separate fluorite from these non-target minerals (Pei et al., 2022). It is relatively easy to separate sulphide minerals from fluorite when using xanthate collectors due to the difference of natural hydrophobicity (Ai et al., 2021; Tang and Chen, 2022). However, when the gangue is barite, calcite or/and quartz, fatty acids or their derivatives are usually utilized as the collector (Liu et al., 2020), and separation between fluorite and these oxidized minerals is difficult (Li et al., 1997), especially calcite, it is impossible to the separation of fluorite from it without the addition of depressants because of the same calcium activated site.

Previous investigations showed that many inhibitors have researched to inhibit the calcite in fluorite flotation, such as starch (Zhu et al., 2021), acid water glass (Zhou et al., 2013), sulfonated lignite and dextrin, etc. (Cui et al., 2020; Li et al., 1994), but the application of some depressants is still limited by the high cost, low solubility, eco-system pollution or/and low selectivity. Furthermore, as the properties of fluorite ore can greatly vary across different locations, a depressant that is effective for the separation

DOI: 10.37190/ppmp/188272

of one type of fluorite ore may not necessarily work for others. Consequently, the separation of fluorite from calcite remains a challenge, with much of the research focusing on the development of novel depressants.

PMAA is a low molecular weight polyelectrolyte that is synthesized by copolymerization of maleic acid and acrylic acid in a certain proportion (Cui et al., 2010), and it has an excellent scale inhibition for calcium carbonate, calcium phosphate and calcium sulfate, and it also can be used as an additive for textile printing/dyeing and papermaking (Zhang et al., 2015; Zhu et al., 2000). As such, Zhang and Li (2002) indicated that PMAA presented an excellent scale inhibition for calcium carbonate but not for calcium fluoride. The chemical composition of calcite is the same as calcium carbonate. Based on this, PMAA might chelate with the calcium sites on the calcite surface that will probably be affecting the calcite flotation, and this might be used for calcite depression while allowing fluorite flotation. However, no reports had concerned the utilization of PMAA for the flotation separation of fluorite from calcite.

Therefore, in this research, the object is to determine if PMAA can be introduced as an effective depressant to depress calcite in fluorite flotation under the collector of NaOl. The flotation of fluorite/calcite and the separation between these two minerals were investigated using micro-flotation and artificial mixture minerals flotation. The action mechanism between reagents and fluorite/calcite surfaces was studied through zeta potential, XPS analysis and computational chemistry.

2. Materials and methods

2.1. Minerals and reagents

The high purity calcite was obtained from Lianyungang, China, and the fluorite fetched from Sijiazhuang, China. Both of the minerals were crushed respectively by hammer, and then the crushed samples were dry ground by ceramic ball mill. After that, the size distribution of +37-74 μm was obtained by sieve for micro-flotation. Chemical analysis plotted the $CaCO_3$ content of calcite, and CaF_2 content of fluorite was over 99.90%, which ensured the purities of these two samples. X-ray diffraction (XRD) was measured (see Fig. 1), which further confirmed the samples purification crystals, which satisfied the requirement of the experiments.

The depressant of PMAA active component with 40% wt was purchased from Shandong Usolf Co., LTD.The PMAA molecular weight is about 3000. The analytical grade of NaOl was the collector in experiments. The molecules of PMAA and NaOl were plotted in Fig. 2. The solution pH was controlled through the diluted HCl and NaOH. The resistivity of ultrapure water was 18.2 MΩ·cm which prepared for the experiments.

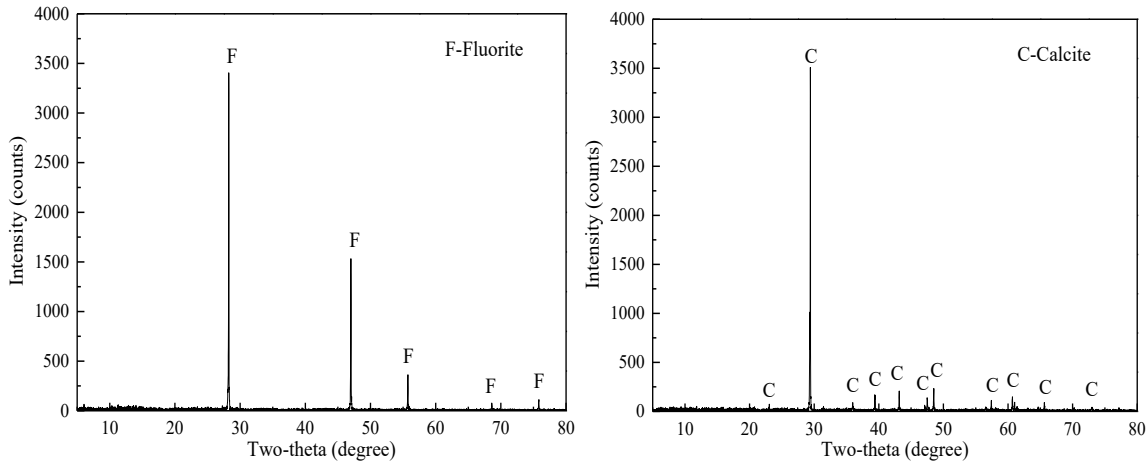

Fig. 1. The XRD patterns of fluorite and calcite minerals

2.2. Micro-flotation tests

XFGC-1600 hanging cell machine can be used for the micro-flotation test. For each preparation, the 40 mL of ultrapure water and 2 g of sample were mixed in the cell, the mixed suspension was conditioned

for 1 min at a fixed pH. After that, PMAA (when required) and NaOl were sequentially added into the solid/liquid mixture using a transfer pipette in order, then recording the pH. Finally, the flotation process was conducted for 5 min. In the single minerals flotation test process, the fluorite or calcite recovery can be ensured by the dry weight of both sink and float products. For artificial minerals mixture flotation, the recovery of sample was obtained by the mass weight of the floated and sunk parts and the content of $CaCO_3$ and /or CaF_2 in the two products. Each test was conducted three times, and value was determined by taking the average. The standard deviation calculation of the results was represented as error bars.

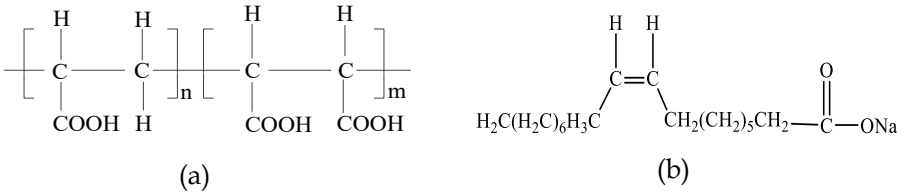

Fig. 2. The molecular structure of PMAA (a) and NaOl (b)

2.3. Zeta potential measurements

The minerals surface electrical properties were represented by zeta potential which determined through Malvern Instrument Nano-ZS90 analyzer (Malvern Instruments Co., LTD, UK). The size fraction of the mineral was ground to -5 μm. For each test, the measured sample was prepared by 40 mg of powders and 80 mL of 1×10^{-3} mol/L KNO_3 solution mixture, and the solid-liquid mixture was treated through a magnetic stirrer under a desired acid-base conditions, then the PMAA or/and NaOl was added in the pulp. After that, the pulp pH value was recorded, then the supernatant collection was used for the zeta potential measurements. To ensure accuracy of data, each sample was tested three times, and the final value was calculated as the average of these measurements. Standard deviations were also presented as error bars.

2.4. XPS analysis

The surface element composition/binding energy of samples were measured through XPS analysis (Thermo Fisher Scientific ESCALAB 250Xi) which operated at 150 W using an Al Kα as the X-ray source. The individual fluorite and calcite were treated at approximately pH 9.0, and then the sample was dried by vacuum drying oven and used for the tests, for comparison, the PMAA treated fluorite and/or calcite was dried and prepared for XPS measurements. To ensured the accurate measurement. The C 1s peak in the experimental data was utilized for energy calibration, and it was situated at 284.80 eV.

2.6. Computational methods and details

Computational chemistry is commonly used to study the interfacial reactions on mineral surfaces, which could be processed in Materials Studio software (Zhang et al., 2022; Azizi and Larachi, 2020). In this work, the CASTEP module firstly used to simulate the crystals properties and electronic structure. DMol3 was then used to calculate the electronic structure and chemical properties of reagent molecules. Finally, the Forcite module was used for molecular dynamics simulation (MDs) to obtain the reaction kinetic behavior between molecules and crystal surfaces, illustrating the interaction mechanism between mineral surface and reagent (Luo et al., 2022; Feng et al., 2023). The structures of fluorite and calcite optimized in the CASTEP module on the basis of our early work (Liu et al., 2023). In fluorite crystal optimization, the exchange-correlation function was truncation energy was fixed at K-point was selected as GGA-PW91, 500 eV and 4×4×4. Regarding the calcite, the exchange-correlation function, cutoff energy, and k-point were GGA-PW91, 400 eV, and 3×3×2, respectively. The PMAA molecule model was built and optimized by means of the Dmol3 module with the exchange-correlation function of B3LYP. A vacuum space of 20 Å was built prior to calculation. After the PMAA was put on the cleavage surface minerals, MDs with the Forcite module applied NVT ensemble. The long-range electrostatic force was addressed by the Ewald summation method, and the van der Waals interactions were used by the atom-based method. The interaction energy (Eads) of the adsorbate at the mineral cleavage surface was determined by Eads=Etot-Esurf-EPMAA, where Esurf and Etot stand represents

the total energy of the material slab in the presence and absence of PMAA adsorption, EDMNS represents the inhibitor the energy of individual PMAA.

Results and discussion

3.1. Floatability of single minerals

To ensure the collecting of NaOl collector, the effect of NaOl concentration on the floatability of two minerals is described in Fig. 3. It could be shown the flotation recoveries of calcite and fluorite markedly rose as the concentration of NaOl increasing. Approximately 90% of the fluorite recovery was obtained when the NaOl addition reached 1.2×10^{-4} mol/L, above that, the fluorite recovery almost unchanged. Fig. 3 also presented that the variation curve of calcite recovery was similar to that of fluorite, and even if the concentration of NaOl exceed 1.0×10^{-4} mol/L, the calcite recovery was slightly more than 90%

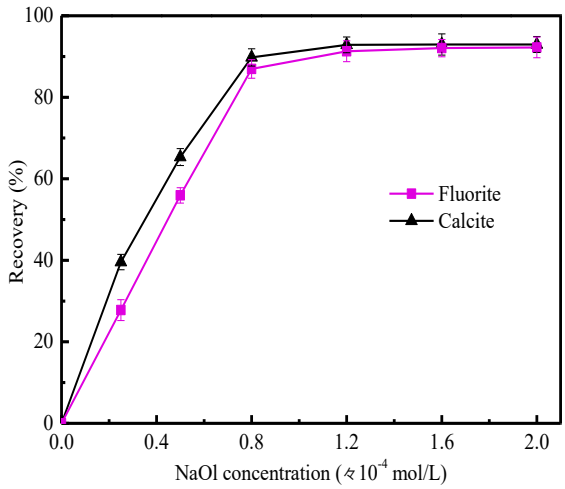

Fig. 3. Impacts of NaOl concentration on the floatability of minerals at pH 9.0

Fig. 4 shows the recoveries of calcite and fluorite when the PMAA was added before NaOl or not. As seen in Fig. 4, the calcite recovery went over 90% in the pH scope of 7-11, and about 90% of the fluorite recovery obtained at pH 7-10. High recoveries of these two minerals illustrated that it is impossible to separate them by adding NaOl alone. When the depressant PMAA was added prior to NaOl, and the recovery of calcite was dramatically dropped, such at pH 9, calcite recovery was around 17%. Interestingly, the fluorite recovery still remained over 80% at pH 8-10 in the presence of when the PMAA was added prior to NaOl.

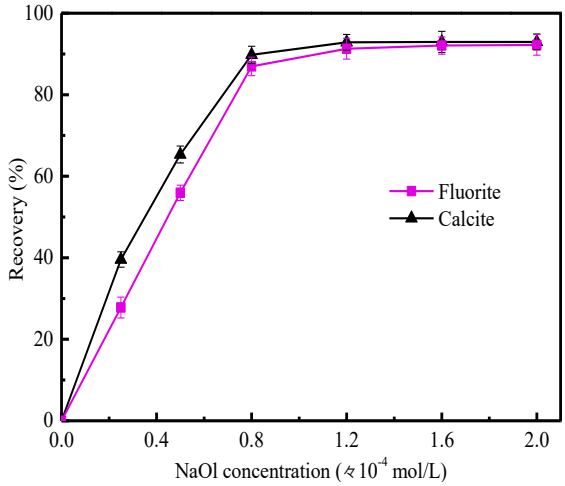

Fig. 4. The impact of pH value on the flotation of minerals (c(PMAA)=10 mg/L; c(NaOl)=1.2×10−4 mol/L)

As shown in Fig. 5. At approximately pH 9.0, the concentration of PMAA noticeably impacted the recoveries of calcite and fluorite when combined with NaOl. The floatability of calcite exhibited a significant drop as the dosage of PMAA increases. Notably, the addition of PMAA reached 12 mg/L, a

difference in the recovery of the two minerals occurred. The calcite recovery was below 10%, illustrating the PMAA entirely depressed the floatability of calcite; in contrast, the flotation recovery of fluorite gradually trending down. However, it's a slow-moving process when the dosage of PMAA was lower than 15 mg/L. It was noteworthy that the recovery of fluorite clearly reduced when the dosage of PMAA exceeded 15 mg/L, suggesting that PMAA could potentially be used as an inhibitor to selectively depress calcite in fluorite flotation. However, the PMAA dosage needs to be controlled and maintained between 10 mg/L to15 mg/L.

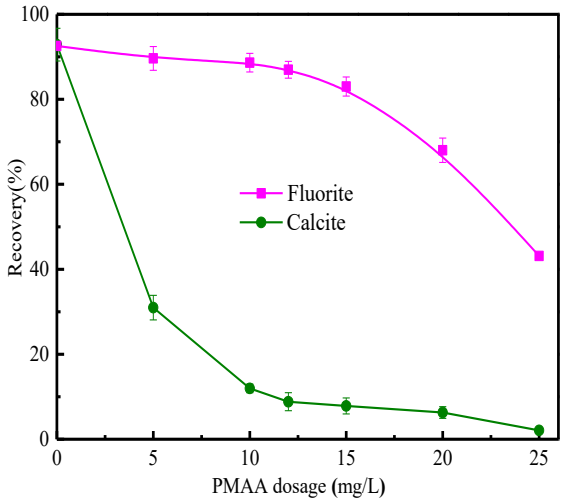

Fig. 5. The impact of PMAA dosage on the flotation of fluorite and calcite at pH 9.0 (c(NaOl): 1.2×10^{-4} mol/L)

To verity the possibility of separating fluorite/calcite with PMAA, the mixture minerals (the fluorite to calcite ratio is 4 to 1) flotation was conducted, and the separation performance is presented in Fig. 6, where the dash line represented the CaF_2 grade in feed. It can be shown that the CaF_2 grade was 80.12% in concentrate by adding individual NaOl, which was closed to that of CaF_2 in raw feed. As 10 mg/L PMAA was introduced in fluorite/calcite system, the CaF_2 grade increased to 92.68%, and recovery decreased to 80.12% in concentrate; however, when the PMAA dosage reached 20 mg/L, the separation efficiency of fluorite from calcite was affected because the recovery of fluorite significantly decreased. Compared to using NaOl alone, the selection of fluorite from calcite clearly improved with PMAA, demonstrating that PMAA could be used as a feasible inhibitor in the fluorite-calcite separation, but the utilization of PMAA dosage need to be controlled.

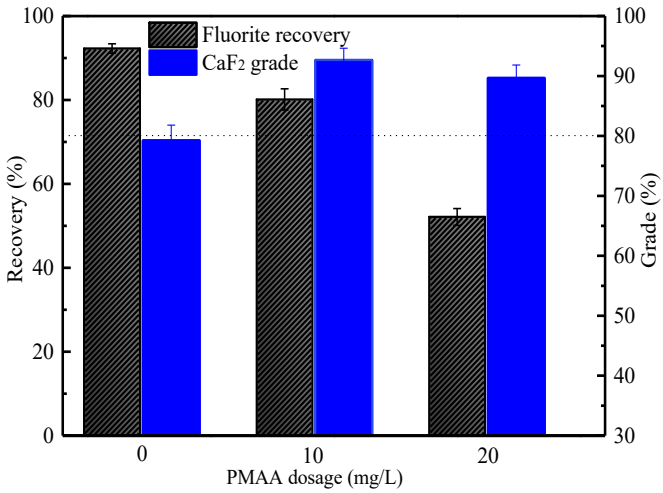

Fig. 6. Flotation results of the fluorite/calcite artificial mixture (pH=9.0, c(NaOl)=1.2×10^{-4} mol/L)

3.2. Zeta potentials results

The zeta potentials measurements were carried out to reflect the variations in the surface charge of fluorite and calcite in the presence and absence of reagents, and the results are exhibited in Fig. 6. It can

be presented that these two samples dropped as the pH value increases without depressant/collector, the isoelectric point of fluorite and calcite was located at approximately pH 7.5 and 9.0, separately, it was closed to the earlier investigations (Liu et al., 2021a; Liu et al., 2021; Shuai et al., 2023). In the presence of NaOl alone, both calcite and fluorite zeta potentials decreased which suggested that interaction occurred between fluorite/calcite and NaOl, this caused no selectively between fluorite and calcite (see Fig. 3 and Fig. 4). Through the treatment of PMAA, the zeta potentials of both fluorite and calcite were also decreased which indicated that PMAA absorbed onto the surfaces of fluorite and calcite, after the treatment of NaOl, the zeta potential of fluorite continued to decrease while that of calcite almost changed. These findings illustrated that NaOl can be absorb onto the PMAA treated fluorite surface while not interacting with calcite surface, leading to a selective depression of calcite when PMAA was added to the fluorite flotation system.

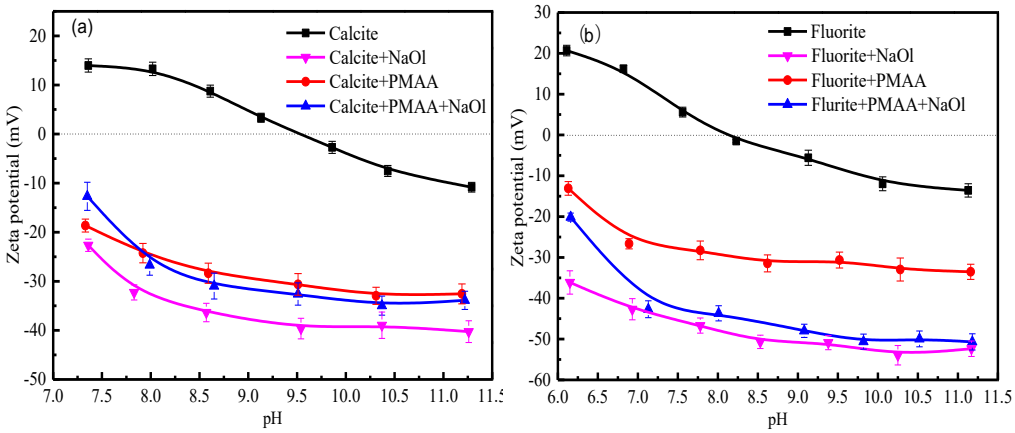

Fig. 7. The impact of pH on the zeta potentials of minerals under different condition (c(PMAA):10 mg/L; c(NaOl): 1.2×10^{-4} mol/L)

3.3. XPS analysis

The XPS measurements were carried out to obtain the fluorite and calcite surfaces elements distribution and their chemical states, and the PMAA treated fluorite and calcite, and the results are presented in Table 1, showing that the element contents of Ca, C, O, and F on the bare fluorite surface were 26.68%, 16.91%, 7.56%, and 48.55%, respectively, when fluorite was treated with PMAA, the content of Ca, C, O, and F changed slightly which indicated the interaction between PMAA and fluorite surface is weak. In the case of calcite, the C, O, and Ca elements contents on it surface was 31.96%, 52.13%, and 15.91%, when the calcite was treated by PMAA, the Ca, C, and O content on its surface changed significantly. Specifically, the C content decreased by 3.16% while the ratio of C/O was increased. This suggested that PMAA with the surface of calcite, possibly replacing carbonate ions,because the C/O of calcite is lower than that of PMAA.

Table 1. The elements contents on the surface of minerals

Samples	Elements contents (%)			
	C	O	F	Ca
Fluorite	16.91	7.56	48.55	26.68
Fluorite+PMAA	18.64	8.45	47.20	25.71
Changing value	1.73	-0.89	1.35	-0.97
Calcite	31.96	52.13	/	15.91
Calcite+PMAA	35.02	49.38	/	15.60
Changing value	3.16	-2.75	/	-0.31

The activated sites of mineral surface act a vital role in minerals flotation. Hence, to further investigate the chemical states of activated calcium site on the two Cabearing minerals surface, the high-resolution Ca 2p spectra for fluorite and calcite with and without PMAA treatment were measured and the results of peak fitting are plotted in Fig. 8 and Fig. 9. Fig. 8a presented two remarkable peaks at 347.80 eV and 351.45 eV was belonged to the Ca 2p3/2 and Ca 2p1/2 of calcium fluorid (Yang et al.,

2020). When the fluorite surface was treated with PMAA, no new fitted peaks appeared besides the peaks of 347.78 eV and 351.36 eV, indicating no effective chemical shift of Ca 2p occurred, and PMAA weakly absorbed on fluorite surface. Regarding the calcite, Fig. 9a plotted that Ca2p3/2 and Ca 2p1/2 peaks of calcium carbonate were observed at the peaks of 346.81 eV and 350.35 eV (Liu et al., 2022, Zhou et al., 2023; Zhang et al., 2023). When calcite surface was treated with PMAA, two new fitted peaks emerged at 347.58 eV and 351.10 eV (Fig. 9b), which corresponded to Ca 2p3/2 and Ca 2p1/2 peaks pf M-COO-Ca (Liu et al., 2021b; Wang et al., 2022). These findings suggested that the PMAA chemically absorbed on the calcite surface mainly through the interaction of its carboxyl groups with calcium ions of calcite.

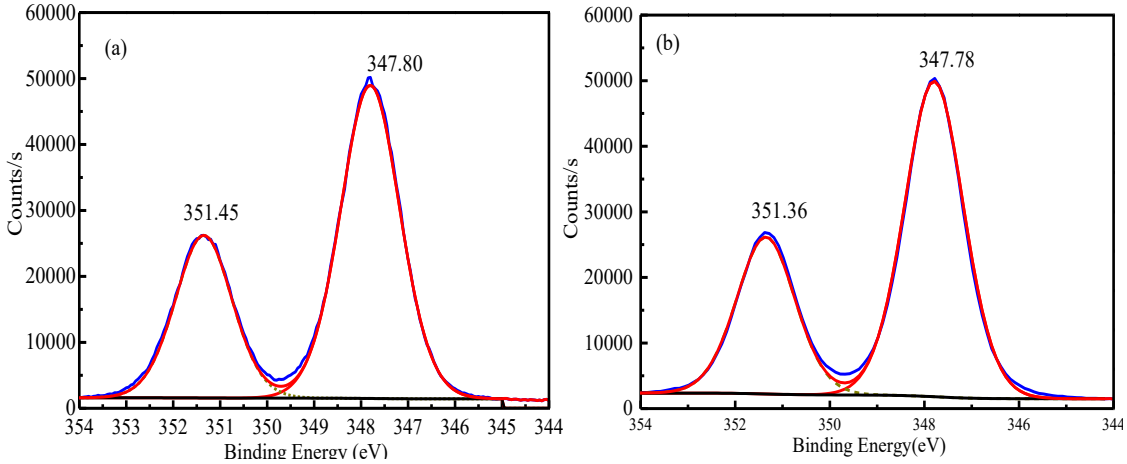

Fig. 8. The peaks of Ca2p spectra of (a) untreated fluorite and after (b) PMAA treated fluorite

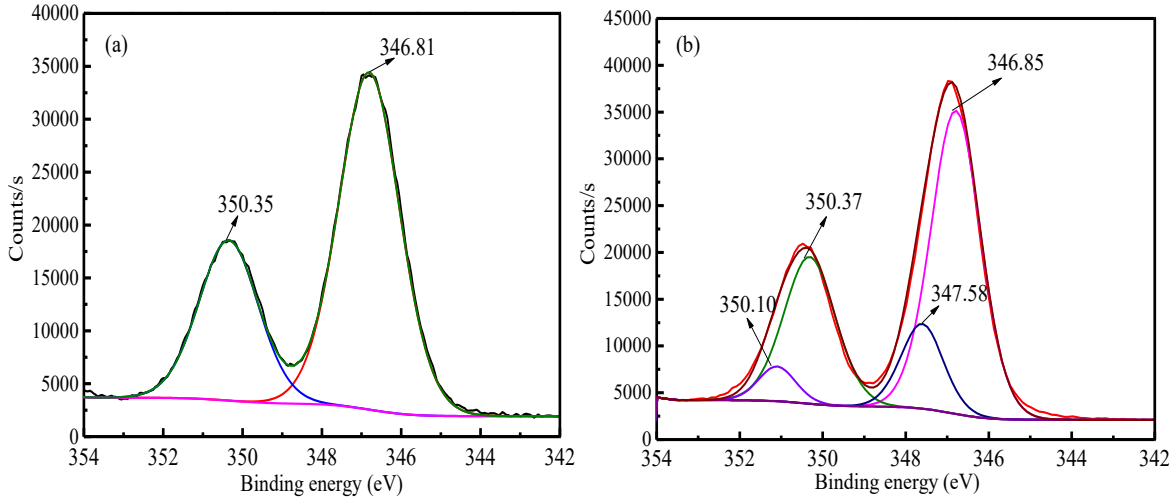

Fig. 9. The peaks of Ca 2p spectra of (a) untreated calcite and (b) PMAA-treated calcite

3.4. Computational results

The previous investigations illustrated that fluorite {111} and calcite {104} cleavage plane are the most stable surface (Gao et al., 2019; Qin et al.2023, Tetteh et al., 2022), calcium ions are exposed on both surfaces of calcite and fluorite. The PMAA molecule was put on top of the fluorite or/and calcite to calculate the adsorption energies of PMAA onto minerals surface. The relative results are shown in Fig. 10. As exhibited, after running equilibrium, the distance between O atom of -COOH group (PMAA) and calcium atom of fluorite surface was 3.381Å and 3.394 Å (see Fig. 10a), respectively, the PMAA had a tendency to escape from the surface which leaded a weak adsorption energy of -29.63 kJ·mol−1. In the case of calcite/PMAA (Fig. 10b), the O atom of -COOH group (PMAA) bonded with the calcium atom on the calcite surface to form four-membered ring, and the two new bonds are 2.410 Å and 2.629 Å, leading to a strong adsorption energy of -128.56 kJ·mol−1. This strong adsorption of PMAA onto calcite implied that NaOl could not interacted with the calcite surface.

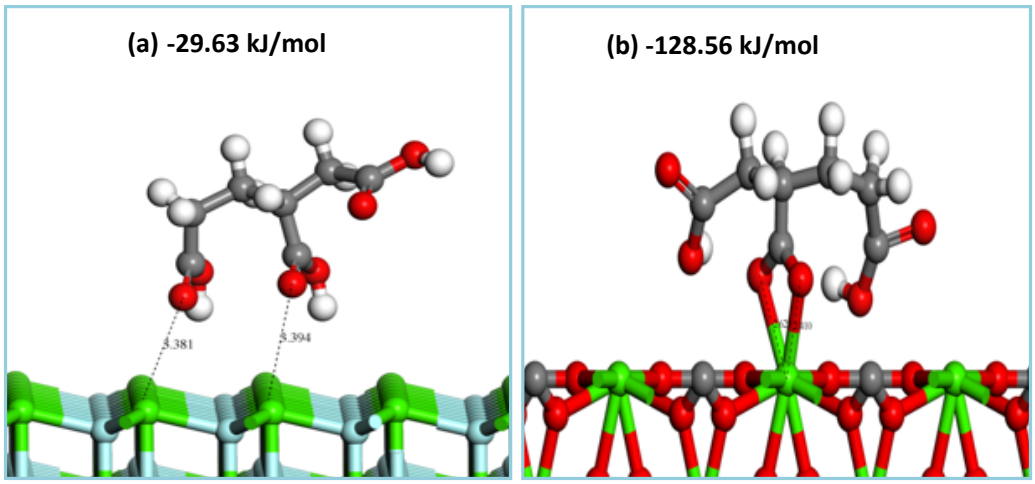

Fig. 10. The adsorption schematic of PMAA on the (a) {111} fluorite surface and (b) {104} calcite plane (Atomic color: Green-Ca, light green- F, red-O, yellow-S, pink-P, grey-C, white-H)

3.4. Discussion

The PMAA co-polymer molecular contains numerous carboxyl groups (see Fig. 2), contributing to its high anioni characteristicsc and hydrophilicity in alkaline solution because of carboxylic acid groups, which allows it to strongly interact with calcium ions (Deng, 2001; Wen et al., 2004). The atoms arrangement of fluorite/calcite surface probably leads to the selective absorption of PMAA in flotation. On the fluorite plane, every two fluoride ions are attached to one calcium ion, and a chemical affinity exists between fluoride ion and calcium ion (Zheng et al., 2018; Pereira et al., 2023), when the fluorite surface is treated with a low concentration of PMAA, the negative fluoride ions probably repel the interaction of the negative PMAA with calcium ions on the fluorite surface due to the electrostatic repulsion, hence the interaction between PMAA and fluorite is weak, but when the concentration of PMAA increased to a certain mount, the negative species of PMAA might enter the stern layer of fluorite surface and interact with calcium ions, that why a low concentration of PMAA can not hinder the NaOl adsorption on fluorite surface while a high concentration of PMAA hinder the NaOl adsorption on it surface, thus causing a difference inhibition performance under different dosage of PMAA for fluorite (see Fig. 5). Regarding the calcite, the {104} plane occurred along two carbonate groups, thereby exposing the calcium site expose on the surface of calcite (Fenter and Sturchio, 2012; Huang et al., 2023; Wang et al., 2021b). However, the radius of CO_3^{2-} is longer than that of F^-, therefore the chemical affinity of Ca^{2+} with CO_3^{2-} is weaker than that of Ca^{2+} with F^-. Hence, in solution, carbonate ions easily enter the liquid phase while calcium ions stay on calcite surface (Liu et al., 2022); after that, the PMAA might easily interact with the exposed calcium ions on calcite surface, hindering the adsorption of NaOl onto calcite surface since no extra activated Ca site was provided on calcite for NaOl interaction. The schematic representation of the interaction mechanism between minerals and reagents is plotted in Fig. 11.

4. Conclusions

The utilization of PMAA polymer as an inhibitor for calcite in fluorite flotation was researched in this work. The micro-flotation tests suggested that the collector NaOl has a good collection for both fluorite and calcite, the PMAA selectively decreased the floatability of calcite within the dosage range of 10~15 mg/L. The artificial minerals mixture flotation ensured that effective separation could be achieved between fluorite and calcite when the NaOl was added after PMAA, but the dosage of PMAA needs to be controlled. Zeta potential results demonstrated that PMAA addition before NaOl hindered the interaction between NaOl and calcite while can not hinder the interaction between NaOl and fluorite. The XPS analysis and MDs confirmed the adsorption of PMAA on the fluorite surface was very weak, but the chemisorption occurred between PMAA and calcite surface, leading to a stably adsorption of PMAA on the calcite surface. The electrostatic interaction between fluorite/calcite surface anion and carboxy group of PMAA probably acted a vital role on the separation of fluorite from calcite.

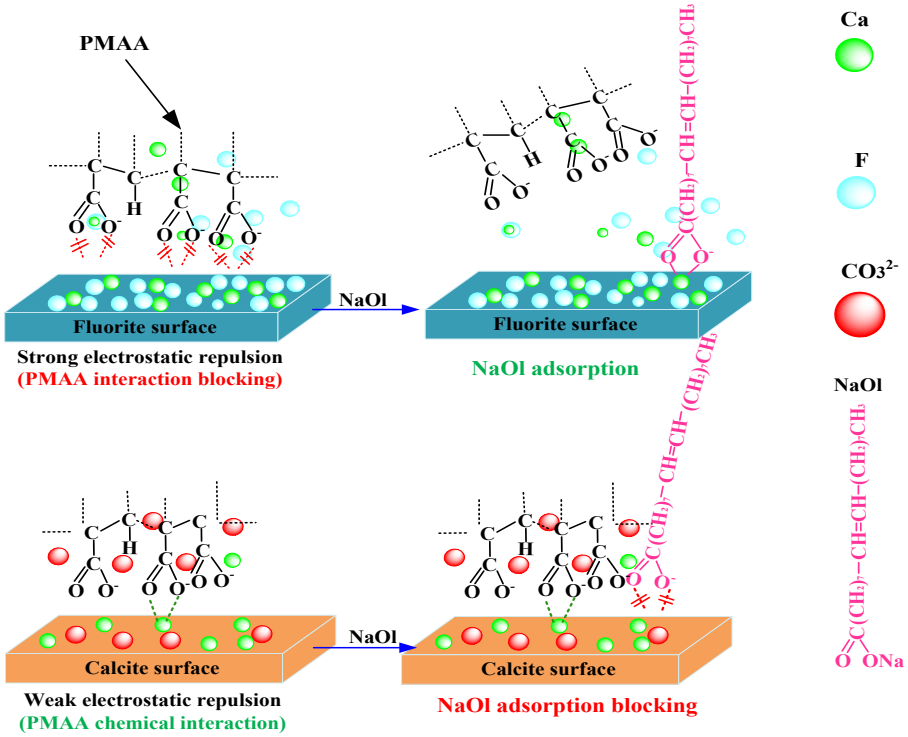

Fig. 11 The schematic interaction mechanism between minerals and reagents

Acknowledgments

The authors acknowledge the support of the National Key Research and Development Program of China (2022YFC2905800, 2022YFE0126800), the National Natural Science Foundation of China (52274269), Major science and technology project of Hubei Province of China (2022ACA004-5), the Research Fund Program of Hubei Key Laboratory of Resources and Eco-Environment Geology (HBREGKFJJ-202307).

References

AI, G., HUANG, K., LIU, C., YANG, S.,2021. *Exploration of amino trimethylene phosphonic acid to eliminate the adverse effect of seawater in molybdenite flotation*. International Journal of Mining Science and Technology, 31(6), 1129-1134.

AZIZI, D., LARACHI., F. 2020. *DFT simulations of pyrite galvanic interactions with bulk, solid-solution and nanoparticle Au occurrences-Insights into gold cyanidation*, Miner. Eng., 149, 106239.

CUI, K., ZOU, X., YUN, L., 2010. *Study on Synthesis of maleic anhydride-acrylic acid copolymer*. Fine Chemicals, 27(2), 179-181 (in Chinese).

CUI, Y., JIAO, F., WEI, Q., WANG, X., Dong, L., 2020. *Flotation separation of fluorite from calcite using sulfonated lignite as depressant*. Separation and Purification Technology. 242(7), 116698.

DENG S., 2001. *Study on coordination chemistry between several new scale inhibitors and scale forming ions in solution.* Tongji University, (Master's thesis), (in Chinese).

FANG, C. J., FENG, Q. M., OU, L.M., XIAO, J., 2014. *Flotation tests on comprehensive recycling of low grade fluorite from tungsten-tailing*. Nonferrous Metals Science and Engineering. 5(2), 72-76 (in Chinese).

FENG, Y., LI, Z.F., CHEN, J.H., CHEN, Y., 2023. *Effect of content and spin state of iron on electronic properties and floatability of iron-bearing sphalerite: A DFT+U study,* International Journal of Mining Science and Technology, 33(12), 1563-1571.

FENTER, P., STURCHIO, N., 2012. *Calcite {104}–water interface structure, revisited*. Geochimica et Cosmochimica Acta, 97, 58-69.

GAO, Z., WANG, C., SUN, W., GAO, Y., KOWALCZUK, P. B., 2021. *Froth flotation of fluorite: a review*. Advances in Colloid and Interface Science, 290, 102382.

GAO, Z., FAN, R., RALSTON, J., SUN, W., HU, Y., 2019. *Surface broken bonds: An efficient way to assess the surface behaviour of fluorite*. Minerals Engineering, 130, 15-23.

GAO, Z., BAI, D., SUN, W., CAO, X., HU. Y., 2015. *Selective flotation of scheelite from calcite and fluorite using a collector mixture*, Minerals Engineering, 72, 23-26

HE, J., SUN, W., ZENG, H., FAN, R., HU, W., GAO, Z., 2022. *Unraveling roles of lead ions in selective flotation of scheelite and fluorite from atomic force microscopy and first-principles calculations*. Minerals Engineering, 179, 107424.

HUANG, Z.Y., KUANG, J.Z., YU.M.M., DING, D., 2023. *Quinic acid as a novel depressant for efficient flotation separation of scheelite from calcite,* Physicochemical Problems of Mineral Processing, 29(2), 166008.

LI, Z.Y., WANG, X.W., XU, C.Y., SUN, T.C., LIU, W.R., WEI, Z.J., 2022. *Effect and mechanism of depressant CK102 on flotation separation of fluorite and dolomite*, Physicochemical Problems of Mineral Processing, 58(3), 145796.

LI, Y., LIU, Q., XU, S., 1994. *Interaction between metal ion components on mineral surface and dextrin (III)─ Flotation separation of fluorite/calcite and fluorite/rutile in the presence of dextrin*. Industrial Minerals & Processing, 6, 23-25 (in Chinese).

LI, Y., DENG, X., XU, S., 1997. *Adsorption characteristics and mechanism of dextrin on barite and fluorite surfaces*, Journal of the Chinese Ceramic Society, 25(3), 317-322.

LIU, C., SONG, S., LI, H., 2019a. *Selective flotation of fluorite from barite using trisodium phosphate as a depressant*. Minerals Engineering, 134, 390-393.

LIU, C., ZHANG, X., ZHENG, Y., REN, Z., YANG, S., 2021. *Utilization of water glass as a dispersant to improve the separation performance of fluorite from barite slimes*. Colloids and Surfaces A. Physicochemical and Engineering Aspects, 635(2), 128036.

LIU, C., ZHU, L., FU, W., CHI, R., LI, H., Yang, S., 2022. *Investigations of amino trimethylene phosphonic acid as a green and efficient depressant for the flotation separation of apatite from calcite*. Minerals Engineering, 181, 107552.

LIU, C., ZHU, Y., HUANG, K., YANG, S., LIANG, Z., 2021a. *Studies of benzyl hydroxamic acid/calcium lignosulphonate addition order in the flotation separation of smithsonite from calcite*. International Journal of Mining Science and Technology, 31(6), 1153-1158.

LIU, C., WANG, X., YANG, S., REN, Z., LI, C., 2021b. *Utilization of polyepoxysuccinic acid as a green depressant for the flotation separation of smithsonite from calcite*. Minerals Engineering, 168, 106933.

LIU, H., KHOSO, S.A., SUN, W., ZHU, Y.G., HAN, H., HU, Y.H., KUANG, J.H., MENG, X.S., ZHANG, Q.P., 2019b. *A novel method for desulfurization and purification of fluorite concentrate using acid leaching and reverse flotation of sulfide*. Journal of Cleaner Production, 209, 1006-1015.

LIU, C., ZHOU, M., XIA, L., FU, W., YANG, S., 2020. *The utilization of citric acid as a depressant for the flotation separation of barite from fluorite*. Minerals Engineering, 156, 106491.

LUO, Y.J., OU, L.M., CHEN, J., ZHANG, G. F., XIA, Y., ZHOU, B., ZHOU, H. *Hydration mechanisms of smithsonite from DFT-D calculations and MDSs*. International Journal of Mining Science and Technology, 2022, 605-613.

PELHAM, L., 1985. *Sources and availability of raw materials for fluorine chemistry*, Journal of Fluorine Chemistry, 30, 1-17

PEI, Q.M., LI, C.L., ZHANG, S.T., ZHOU, H., LIANG, Y., WANG, L., LI, S.L., CAO, H.W., 2022. *Vein-type fluorite mineralization of the linxi district in the great xing'an range, northeast china: insights from geochronology, mineral geochemistry, fluid inclusion and stable isotope systematics*. Ore Geology Reviews, 142, 104708.

PEREIRA, L., KUPKA, N., HOANG, D.H., MICHAUX, B., SAQURAN, S., EBERT, D., RUDOLPH, M. 2023. *On the impact of grinding conditions in the flotation of semi-soluble salt-type mineral-containing ores driven by surface or particle geometry effects?* International Journal of Mining Science and Technology, 33(7), 855-872.

QIN, W.Q., HU, J.J., ZHU.H.L., JAIO, F., JIA, W.H., HAN, J.W., CHEN, C., 2023. *Effect of depressants on flotation separation of magnesite from dolomite and calcite,* International Journal of Mining Science and Technology, 33(1): 83-89.

SHUAI, S.Y., HUANG, Z.Q., BUROV, V.E., POILOV, V. Z., LI, F.X., WANG, H.L., LIU, R.K., ZHANG, S.Y., CHENG, C., LI, Y.W., YU, X.Y., HE, G.C., FU, W., 2023. *Flotation separation of wolframite from calcite using a new trisiloxane surfactant as collector,* International Journal of Mining Science and Technology, 33(3), 379-387.

TANG, X., CHEN, Y., 2022. *A review of flotation and selective separation of pyrrhotite: A perspective from crystal structures.* International Journal of Mining Science and Technology, 32(4), 847-863.

TANG, Y., 2010. *Current Situation of Fluorite Mineral Resources and Its Utilization and Development Strategy*, Organo-Fluorine Industry, 1, 51-55 (in Chinese).

TETTEH, J., BAI, S., KUBELKA, J., PIRI, M., 2022. *Surfactant-induced wettability reversal on oil-wet calcite surfaces: experimentation and molecular dynamics simulations with scaled-charges*. Journal of Colloid and Interface Science,609, 890-900.

SEREDENKO, V.A., FILIPPOV, E.A., SHATALOV, V.V., DEDOV, A.S., RODIN, V.I., 1992. *A study of chemical interactions in the manufacture of hydrofluoric acid by high-temperature hydrolysis*. Journal of Fluorine Chemistry, 58(2-3), 325-325.

WANG, L., LYU, W., ZHOU, W., ZHANG, H., 2022. *The role of sodium phytate in the flotation separation of smithsonite from calcite,* Minerals Engineering, 187, 107775.

WANG, Y.C., ZHANG, Z.T. 2010. *Self-assembly of calcium ions with baicalein sulfonate.* Chinese Journal of Spectroscopy Laboratory, 27(01), 43-48(in Chinese).

WANG, Z., REN, Z., GAO, H., GAO, Z., XU, L., ZHU, X., LIU, Y., 2021a. *Effect of active substance content and molecular weight of petroleum sulfonate on fluorite flotation: molecular dynamics simulation*. Minerals Engineering, 174, 107257.

WANG, C., REN, S., SUN, W., WU, S.H., TAO, L.M., DUAN, H., WANG, J.J., GAO, Z.Y., 2021b. *Selective flotation of scheelite from calcite using a novel self-assembled collector*, Minerals Engineering, 171, 107120.

WEN, R., DENG, S, ZHU, Z., WEI, F., ZHANG, Y., 2004. *Studies on complexation of ATMP, PBTCA, PAA and PMAAA with Ca^{2+} in aqueous solutions.* Chemical Research in Chinese Universities, 20(001), 36-39.

YANG, S., XU, Y., LIU, C., HUANG, L., HUANG, Z., LI, H., 2020. *The anionic flotation of fluorite from barite using gelatinized starch as the depressant.* Colloids and Surfaces A: Physicochemical and Engineering Aspects, 597,124794

YE, Z.P., HE, G.W., 2005. *New technology on comprehensive recovery of fluorite from shizhuyuan wolframite flotation tailings.* Nonferrous Metals,57, 70-72 (in Chinese).

YE, L., LU, Y.C., 2021. *Intensifying fine-grained fluorite flotation process with a combination of in-situ modification and liquid-gas microdispersion*. Separation and Purification Technology, 257, 117982

ZHANG, B., LI F., 2022. *Versatile scale inhibition of polyepoxysuccinic acid*. Industrial Water Treatment, 22(9), 21-24 (in Chinese).

ZHANG, C.L., YE, Y.L., YANG, N., YANG, Y.2015. *Performance tests and kinetics research on three kinds of scale inhibitors*, Industrial Water Treatment, 35(9), 50-53 (in Chinese).

ZHANG, H., SUN, W., ZHANG, C., HE, J., CHEN, D., ZHU, Y. 2022. *Adsorption performance and mechanism of the commonly used collectors with Oxygen-containing functional group on the ilmenite surface: A DFT stud*y, J. Mol. Liq., 346, 117829.

ZHENG, R., REN, Z., GAO, H., CHEN, Z., QIAN, Y., LI, Y., 2018. *Effects of crystal chemistry on sodium oleate adsorption on fluorite surface investigated by molecular dynamics simulation*. Minerals Engineering, 124, 77-85.

ZHOU, W., MORENO, J., TORRES, R., VALLE, H., SONG, S., 2013. *Flotation of fluorite from ores by using acidized water glass as depressant.* Minerals Engineering, 45, 142-145.

ZHOU, H.P., WU, H.D., GUO, J.F., TANG, X.K., HUANG, W., LUO, X.P., 2023. *Application of Diethylenetriaminepenta pentasodium salt as an eco-friendly depressant to effectively improve the flotation separation of scheelite and calcite*, Physicochemical Problems of Mineral Processing, 59(9), 174718.

ZHU, W., PAN, J., YU, X., HE, G., LIU, T., 2021. *The flotation separation of fluorite from calcite using hydroxypropyl starch as a depressant.* Colloids and Surfaces A. Physicochemical and Engineering Aspects, 98, 126168.

ZHU, Z.L., ZHANG, R.B., SU, Y.D., 2000. *Kinetic study of inhibition mechanism of PBTCA and AA-MA copolymer on $CaCO_3$ scale*, Industrial Water Treatment, 20(2), 20-23 (in Chinese).